Electronic Supplementary Information

Quasi-one-dimensional BiSeX (X = Br , I) semiconductors as promising thermoelectric materials with anisotropic transport properties

Yunping Yang, Kang Zhang, Hongkuan Yuan, Hong Chen*

School of Physical Science and Technology, Southwest University, Chongqing 400715, China
*Corresponding author. E-mail: chenh@swu.edu.cn

1. Intrinsic carrier concentration

Based on the Fermi-Dirac distribution and density of states (DOS), we calculated the intrinsic carrier concentration of the BiSeX (X = Br, I) with the following expressions:

$$n_0 = \int_{E_F}^{+\infty} \rho_c(E) f(E) dE, \quad \text{(S1)}$$

$$\rho_0 = \int_{-\infty}^{E_F} \rho_v(E)[1 - f(E) dE], \quad \text{(S2)}$$

$$f(E) = \frac{1}{e^{\frac{E-E_F}{k_B T}} + 1}, \quad \text{(S3)}$$

where E_F is the Fermi level, k_B is the Boltzmann constant, $f(E)$ represents the electron occupation probability, and $1 - f(E)$ corresponds to the hole occupation probability. Additionally, $\rho_c(E)$ and $\rho_v(E)$ denote the density of states (DOS) of the conduction and valence bands, respectively.

2. Convergence test on the lattice thermal conductivity

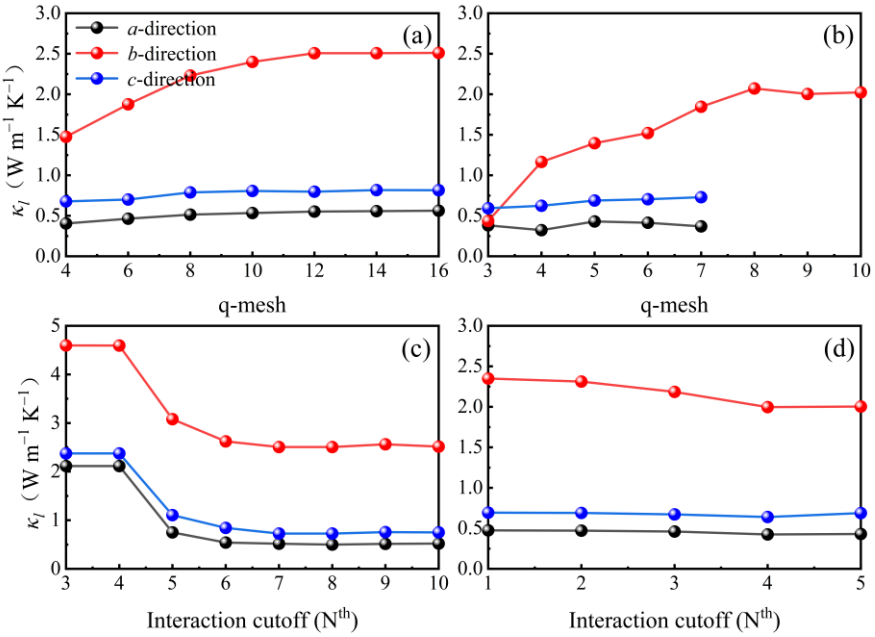

Fig. S1 Convergence tests for (a) the 3ph (b) 3+4ph q-mesh, and (c) and (d) cutoff values for the cubic and quartic force constant interactions in the thermal conductivity of BiSeI.

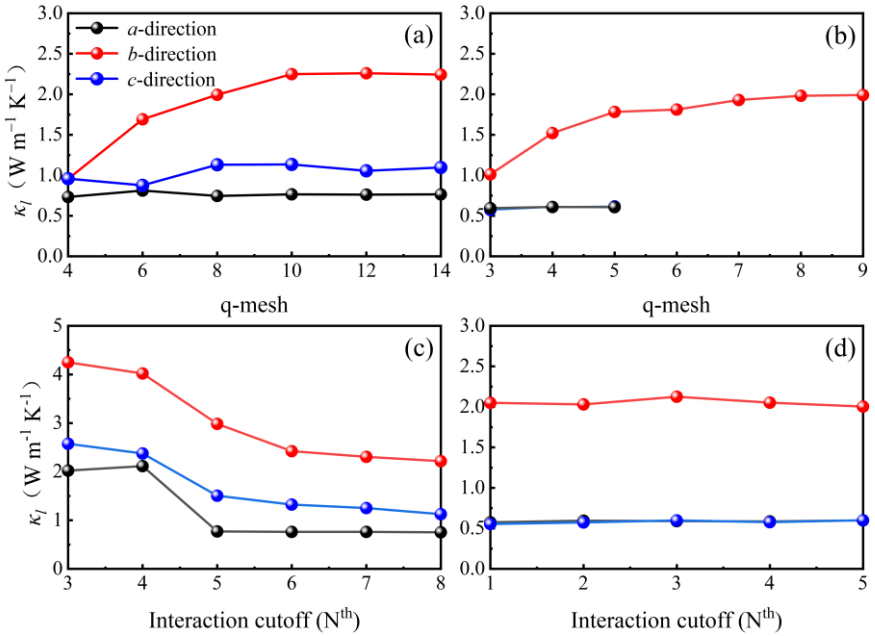

Fig. S2 Convergence tests for (a) the 3ph (b) 3+4ph q-mesh, and (c) and (d) cutoff values for the cubic and quartic force constant interactions in the thermal conductivity of BiSeBr

3. Convergence test of the phonon spectra with respect to the supercell size

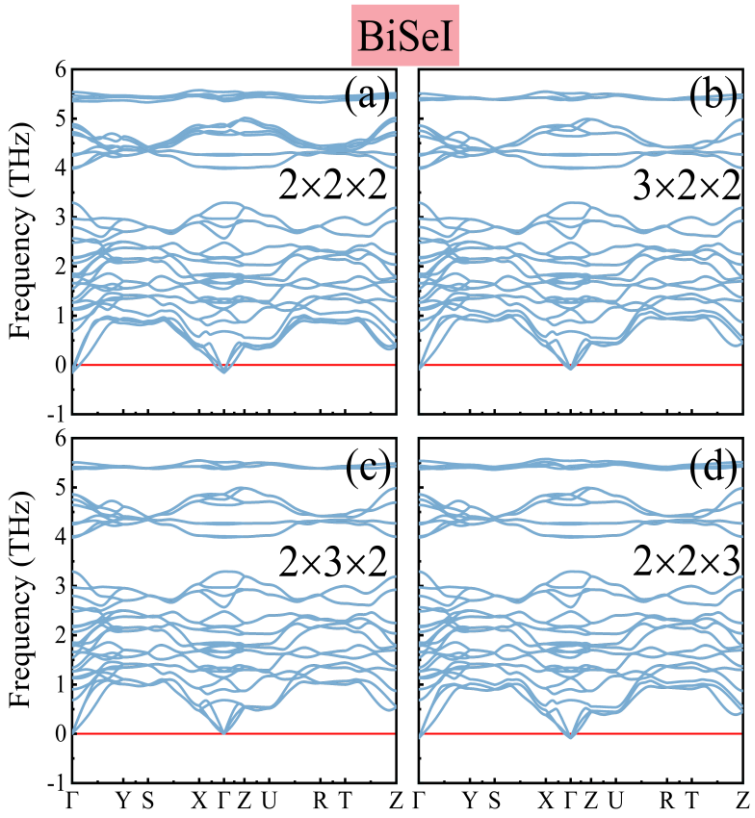

Fig S3 Convergence test of the phonon spectra with respect to supercell size of (a) 2×2×2, (b) 3×2×2, (c) 2×3×2, and (d) 2×2×3 supercells for BiSeI.

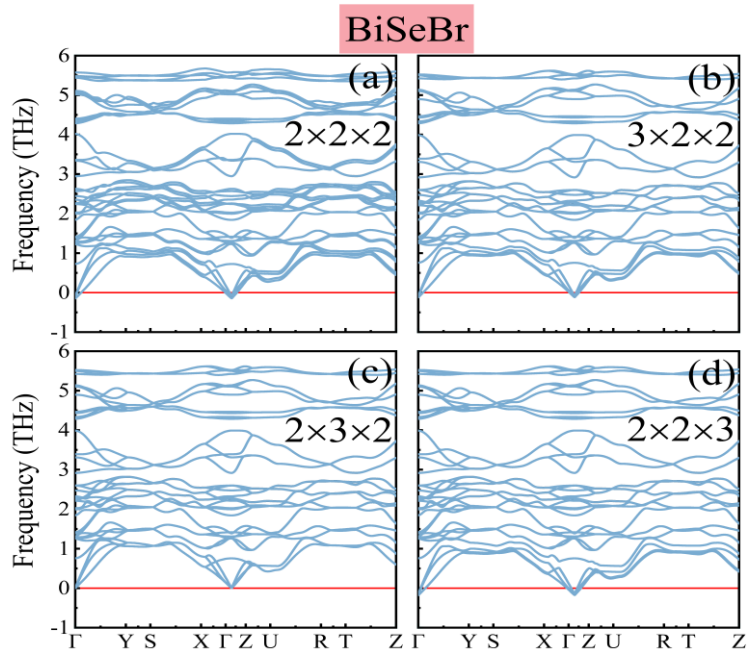

Fig. S4 Convergence test of the phonon spectra with respect to the supercell size (a) 2×2×2, (b) 3×2×2, (c) 2×3×2, and (d) 2×2×3 supercells for BiSeBr.

4. The *ab initio* molecular dynamics (AIMD) simulations

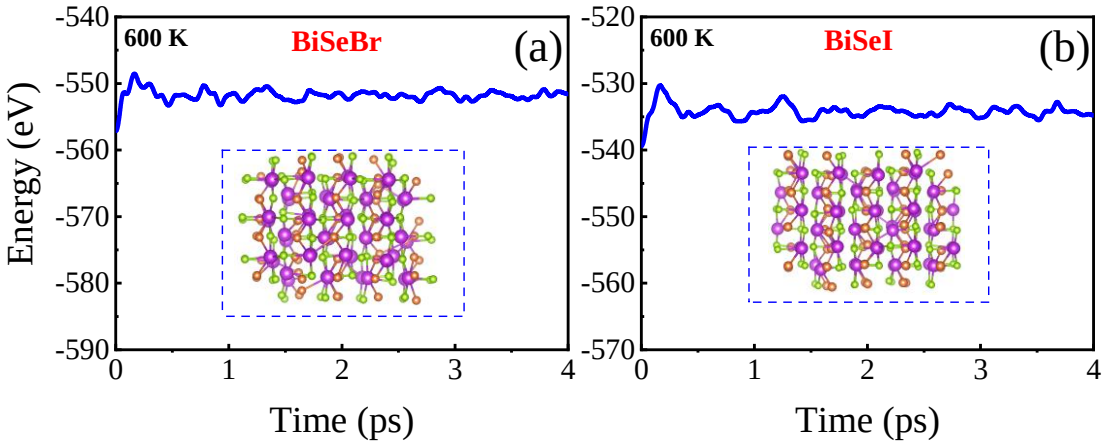

Fig. S5 The energy of the BiSeX (X = Br/I) by AIMD simulation at 600 K.

5. Carrier mobility in intrinsic carrier concentrations

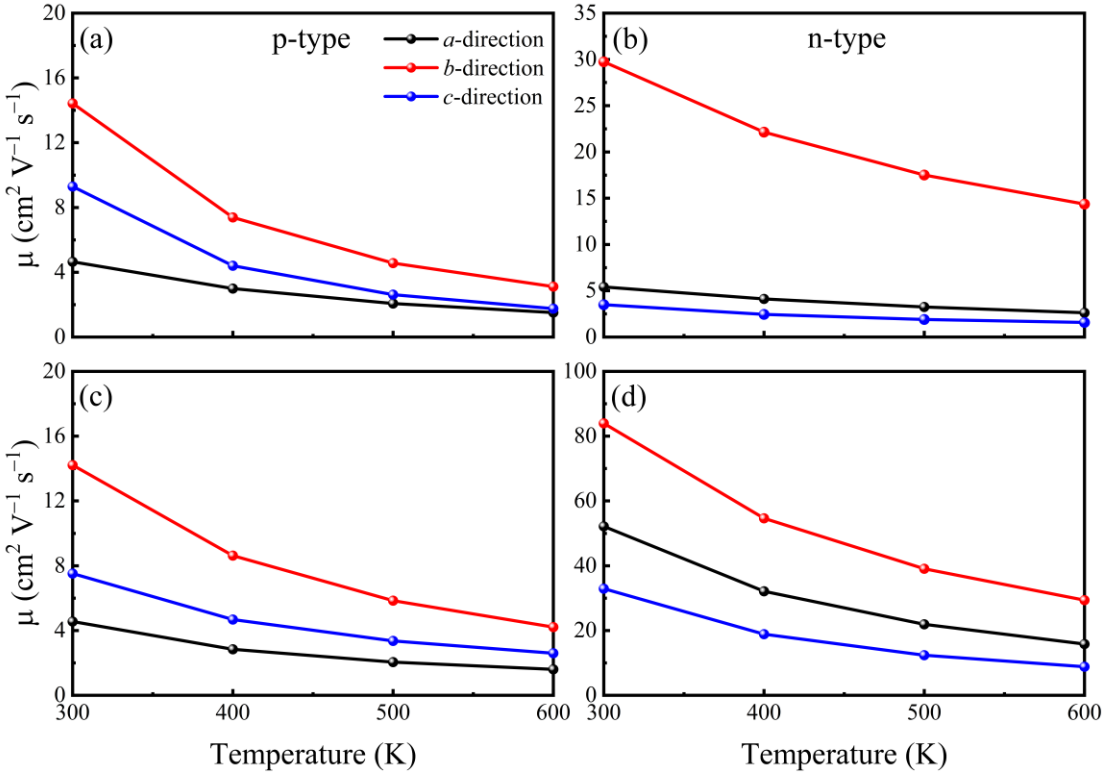

Fig. S6 Calculated temperature-dependent carrier mobility for p- and n-type BiSeI (a, b) and BiSeBr (c, d) in intrinsic carrier concentrations. Black, red, and blue lines indicate transport along the *a*-, *b*-, and *c*-axes, respectively.

6. Calculated Born effective charge tensors for the different atoms in BiSeI and BiSeBr.

Table S1 Born effective charge tensors Z_{κ}^{*} (in units of *e*) for the different atoms in BiSeI and BiSeBr.

Compound	Atom	Born effective charge tensor $Z_{\kappa}^{*}=\begin{pmatrix} Z_{xx}^{*} & Z_{xy}^{*} & Z_{xz}^{*} \\ Z_{yx}^{*} & Z_{yy}^{*} & Z_{yz}^{*} \\ Z_{zx}^{*} & Z_{zy}^{*} & Z_{zz}^{*} \end{pmatrix}$
BiSeI	Bi	$\begin{pmatrix} 2.93 & 0 & -0.11 \\ 0 & 6.11 & 0 \\ -1.17 & 0 & 3.98 \end{pmatrix}$
BiSeI	Se	$\begin{pmatrix} -1.14 & 0 & -0.11 \\ 0 & -3.00 & 0 \\ 0.77 & 0 & -1.74 \end{pmatrix}$
BiSeI	I	$\begin{pmatrix} -1.79 & 0 & -0.80 \\ 0 & -3.11 & 0 \\ -1.13 & 0 & -2.23 \end{pmatrix}$
BiSeBr	Bi	$\begin{pmatrix} 2.16 & 0 & 0.10 \\ 0 & 5.72 & 0 \\ 0.89 & 0 & 3.35 \end{pmatrix}$
BiSeBr	Se	$\begin{pmatrix} -0.72 & 0 & 0.10 \\ 0 & -2.65 & 0 \\ -0.58 & 0 & -1.39 \end{pmatrix}$
BiSeBr	Br	$\begin{pmatrix} -1.44 & 0 & -0.71 \\ 0 & -3.07 & 0 \\ -1.08 & 0 & -1.97 \end{pmatrix}$

7. Electrical transport properties and the dimensional less merit of figure (zT) of BiSeI under intrinsic carrier concentrations at different temperatures

Table S2 Electrical transport parameters (σ, S, κ_e, and PF) and the dimensional less merit of figure (zT) of BiSeI under intrinsic carrier concentrations at different temperatures

T(K)	Direction	Type	300 K	400 K	500 K	600 K
Intrinsic carrier concentration		n	4.29×10^{17}	1.90×10^{18}	3.18×10^{18}	4.27×10^{18}
		p	2.36×10^{17}	1.41×10^{18}	4.81×10^{18}	1.19×10^{19}
σ (Ω^{-1} m^{-1})	a	n	37.28	125.30	165.43	179.84
		p	17.57	67.55	159.46	288.69
	b	n	204.49	673.86	892.18	982.24
		p	54.55	166.96	351.72	594.00
	c	n	24.06	74.61	96.83	107.76
		p	35.14	99.53	201.94	334.86
s (μV K^{-1})	a	n	−646.17	−539.21	−508.37	−493.92
		p	714.28	605.07	523.83	485.37
	b	n	−633.55	−535.36	−511.12	−501.08
		p	631.46	550.59	502.31	473.31
	c	n	−614.40	−523.36	−510.10	−511.89
		p	611.92	535.89	488.58	457.30
κ_e (W m^{-1} K^{-1})	a	n	1.66×10^{-4}	6.46×10^{-4}	9.57×10^{-4}	1.19×10^{-3}
		p	9.41×10^{-5}	4.08×10^{-4}	1.24×10^{-3}	2.86×10^{-3}

	b	n	9.84×10^{-4}	4.05×10^{-3}	6.26×10^{-3}	7.87×10^{-3}
		p	2.98×10^{-4}	1.33×10^{-3}	3.69×10^{-3}	8.25×10^{-3}
	c	n	1.10×10^{-4}	5.13×10^{-4}	9.07×10^{-4}	1.29×10^{-3}
		p	1.79×10^{-4}	7.75×10^{-4}	2.03×10^{-3}	6.24×10^{-3}
PF ($W\ m^{-1}\ K^{-2}$)	a	n	1.56×10^{-5}	3.64×10^{-5}	4.28×10^{-5}	4.39×10^{-5}
		p	8.97×10^{-6}	2.47×10^{-5}	4.53×10^{-5}	6.80×10^{-5}
	b	n	8.21×10^{-5}	1.93×10^{-4}	2.33×10^{-4}	2.47×10^{-4}
		p	2.17×10^{-5}	5.06×10^{-5}	8.87×10^{-5}	1.33×10^{-4}
	c	n	9.08×10^{-6}	2.04×10^{-5}	2.52×10^{-5}	2.82×10^{-5}
		p	1.32×10^{-5}	2.86×10^{-5}	4.82×10^{-5}	7.00×10^{-4}
zT	a	n	0.010	0.038	0.070	0.097
		p	0.006	0.026	0.074	0.149
	b	n	0.012	0.053	0.103	0.158
		p	0.003	0.014	0.039	0.085
	c	n	0.004	0.017	0.033	0.058
		p	0.006	0.024	0.064	0.141

Table S3 Electrical transport parameters (σ, S, κ_e, and PF) and the dimensional less merit of figure (zT) of BiSeBr under intrinsic carrier concentrations at different temperatures

T(K)	Direction	type	300 K	400 K	500 K	600 K
Intrinsic carrier concentration		n	4.52×10^{17}	1.86×10^{18}	3.08×10^{18}	5.23×10^{18}
		p	2.38×10^{17}	1.36×10^{18}	4.51×10^{18}	1.11×10^{19}
σ (Ω^{-1} m^{-1})	a	n	330.00	872.67	1025.59	1303.15
		p	35.34	143.20	341.56	620.75
	b	n	790.34	2191.28	2637.72	3385.32
		p	50.86	182.15	417.71	760.56
	c	n	143.46	495.03	704.63	1031.12
		p	47.94	158.12	348.72	617.71
s (μV K^{-1})	a	n	−488.17	−412.40	−406.65	−393.87
		p	732.42.	609.67	527.98	470.45
	b	n	−499.44	−421.45	−411.65	−392.87
		p	684.99	588.36	523.98	477.04
	c	n	−563.27	−488.28	−475.57	−452.31
		p	655.98	570.71	510.59	464.43
κ_e (m^{-1} K^{-1})	a	n	1.66×10^{-3}	6.23×10^{-3}	9.66×10^{-3}	1.50×10^{-2}
		p	1.66×10^{-4}	7.34×10^{-4}	2.02×10^{-3}	4.53×10^{-3}
	b	n	4.23×10^{-3}	1.57×10^{-2}	2.26×10^{-2}	3.24×10^{-2}
		p	2.97×10^{-4}	1.30×10^{-4}	3.53×10^{-3}	7.70×10^{-3}
	c	n	1.07×10^{-3}	4.65×10^{-3}	7.44×10^{-3}	1.15×10^{-3}

		p	2.87×10^{-4}	1.18×10^{-3}	2.92×10^{-3}	5.82×10^{-3}
PF ($W\ m^{-1}\ K^{-2}$)	a	n	7.86×10^{-5}	1.48×10^{-4}	1.70×10^{-4}	2.02×10^{-4}
		p	1.90×10^{-5}	5.32×10^{-5}	9.52×10^{-5}	1.37×10^{-4}
	b	n	1.97×10^{-4}	3.89×10^{-4}	4.47×10^{-4}	5.23×10^{-4}
		p	2.39×10^{-5}	6.31×10^{-5}	1.15×10^{-4}	1.73×10^{-4}
	c	n	4.55×10^{-4}	1.18×10^{-4}	1.59×10^{-4}	2.11×10^{-4}
		p	2.06×10^{-5}	5.15×10^{-5}	9.09×10^{-5}	1.33×10^{-4}
zT	a	n	0.040	0.123	0.234	0.354
		p	0.010	0.045	0.134	0.248
	b	n	0.029	0.102	0.182	0.300
		p	0.004	0.017	0.047	0.102
	c	n	0.024	0.108	0.277	0.382
		p	0.011	0.048	0.131	0.245